

Electromagnetic force distribution computations due to switching surge in disc-type winding

Nurul Farahwahida Md Yasid¹, Norhafiz Azis^{1,2}, Mohd Fairouz Mohd Yousof³, Jasronita Jasni¹,
Mohd Aizam Talib⁴, Avinash Srikanta Murthy⁵

¹Advanced Lightning, Power and Energy Research Centre (ALPER), Faculty of Engineering, Universiti Putra Malaysia, Selangor, Malaysia

²Institute of Nanoscience and Nanotechnology (ION2), Universiti Putra Malaysia, Selangor, Malaysia

³Faculty of Electrical and Electronics Engineering, Universiti Tun Hussein Onn Malaysia, Johor, Malaysia

⁴TNB Labs Sdn. Bhd, Selangor, Malaysia

⁵Transformer Technology Centre, Hitachi Energy, Vadodara, India

Article Info

Article history:

Received Aug 16, 2022

Revised Jan 6, 2023

Accepted Jan 10, 2023

Keywords:

Disc winding

Electromagnetic force

Switching surge

Transformer

Transient

ABSTRACT

This manuscript discusses the computation of electromagnetic forces on a disc-type winding due to a standard switching impulse (SSI). First, the resistances, inductances and capacitances (RLC) of a 30 MVA, 33/11 kV disc-type distribution transformer were estimated to obtain the winding equivalent circuit. The transient voltage waveforms for each of the disc layers and corresponding resonances of the windings under the SSI were then obtained in time domains. Next, the axial and radial force distributions in the disc winding due to the SSI were computed. The forces on each disc layer and along the disc windings due to the SSI were computed based on the analytical and numerical methods via the finite element method (FEM) respectively. The non-uniform switching impulse voltage distribution results in non-uniform force distribution along the disc winding. The magnitude of the axially directed force on the disc winding is found to be higher as compared to the radially directed force.

This is an open access article under the [CC BY-SA](https://creativecommons.org/licenses/by-sa/4.0/) license.



Corresponding Author:

Norhafiz Azis

Advanced Lightning, Power and Energy Research Centre (ALPER), Faculty of Engineering

Universiti Putra Malaysia

43400 Serdang, Selangor, Malaysia

Email: norhafiz@upm.edu.my

1. INTRODUCTION

The overvoltages in the power system can be categorized into 2 types, which are external and internal overvoltages. The most common and severe external overvoltage is the lightning surge. The internal overvoltages generated from the electromagnetic interactions between its components are the switching and temporary surges. The presence of switching overvoltages in the transmission and distribution networks can affect the reliability of the transformers [1]. Switching overvoltage can be caused by routine operations, sudden changes in load, connection or disconnection of sections of the network and interruption of short-circuit current. It has long damped oscillating tail duration due to the electromagnetic transient and wave caused by the sudden changes in system operations [2]. The standard switching impulse (SSI) has a wavefront, T_P of 250 μ s and wave tail, T_2 of 2500 μ s as per IEC 60060-1 [3].

The SSI can generate oscillations along the winding and causes abnormal electromagnetic stresses not only to the turn-to-turn but also in section-to-section winding insulation. It can also affect the linearity of the voltage distributions [4]. The magnitude of the switching impulses is approximately 4 to 5 times the nominal

system voltage [5]. Transformers should be able to withstand a series of electromagnetic forces during its operation. However, the cumulative stresses and forces due to the repeating switching surges on the winding can be severe and cause deviation in its electrical and mechanical characteristics. The electromagnetic forces are generated through the reactions between the leakage fluxes and current passing along the transformer windings. These forces are in axial and radial directions correspondingly to the leakage fluxes along the windings that are distributed in these components [6], [7].

The transients on transformer windings based on equivalent circuits and experimental models have been previously investigated in [8], [9]. Other studies have utilized the geometrical models of transformers via simulations and experimental setups to study similar effects [10]–[13]. These methods involve with a number of approximations due to the difficulties to obtain the transformer parameters since it involves with complex modelling of winding equivalent circuit. Multi-conductor transmission line (MTL) model approach was proposed to investigate the helical winding and continuous winding structures [14], [15]. The model involves the assumption that a pair of coils can be represented as a single capacitance. In recent years, electromagnetic models based on finite element method (FEM) have been introduced to support the modelling limitations on the geometrical and equivalent circuit models [16]–[19]. The transformer windings electromagnetic force measurements have been carried out in [20]–[23] with several simplifications and assumptions. FEM is found to be feasible for analysis of the electrical and mechanical damages on the windings [23]–[25]. FEM can model the actual capacitances between any two conductors in much more detail as compared to the MTL model. The FEM able to analyse the transient phenomenon based on the parameters that are computed from the transformer winding design information. In addition, the electromagnetic force of windings depends mainly on the transformer winding geometrical designs which in turn provides analysis closer to physical characteristics than the other modelling methods [26], [27].

Previous FEM studies mainly analyse the magnetic field distribution and electromagnetic force analysis to estimate the forces experienced by the windings under transient conditions. The winding model is quite general, which is only demonstrated as core-type transformers and constructed as layer windings [28]–[32]. General designs of low voltage (LV) and high voltage (HV) winding models were evaluated in [33]–[35]. Currently, there is limited work and understanding on the disc-type winding especially related to the electromagnetic force analysis to estimate the forces subjected to the winding. Comprehensive assessment is necessary to study the electromagnetic force distribution in the disc winding model design. This study can provide information on the electromagnetic force distributions on a winding model with detail disc winding configurations whereby the stress prone zone can be pinpointed.

In this study, the electromagnetic force distribution on HV winding of a 30 MVA, 33/11 kV disc type transformer due to SSI is examined. The first section discusses the computation of the resistances, inductances and capacitances (RLC) elements of the HV disc winding, which is utilized as input data for the winding equivalent circuit model to obtain the transient resonances. The second section describes the simulation of the SSI waveform through a switching impulse generator circuit and it is applied as the excitation on the disc winding model to obtain the electromagnetic forces in FEM. The third section presents the computation of the electromagnetic forces on each disc layer based on analytical method and the overall electromagnetic forces subjected to the winding using the numerical method. The contribution of this study is the examination of electromagnetic forces phenomenon on a disc-type winding due to standard switching surge based on analysis of detail disc winding configurations.

2. RESEARCH METHOD

A 30 MVA, 33/11 kV Dyn11 transformer was examined in this study. The HV and LV winding's nominal voltages are 34.5 and 13.8 kV. The HV and LV windings have BILs of 200 kV and 110 kV respectively. An assumption was made for the 33 kV winding whereby it was solidly grounded and the 13.8 kV winding was low resistance grounded. The crest voltage of 165 kV for the SSI was set below the rated BIL of the HV winding with a protection margin of 21%. Only the 8 topmost HV disc windings were examined based on the assumption that the switching surge normally affected the outer HV winding. This study only discusses the HV disc winding since the magnetic flux that affects the electromagnetic forces and stresses primarily occurs on the corresponding winding.

2.1. The standard switching impulse generation

The impulse waveshape can be generated with a combination of a series RLC circuit under over damped condition. Figure 1 shows the SSI of 250/2500 μ s that was generated by using the impulse generator circuit [36]. The generator Simulink circuit is demonstrated in Figure 1(a) and the 165 kV magnitude SSI waveform is presented in Figure 1(b). The impulse generator circuit specification for the SSI is shown in Table 1.

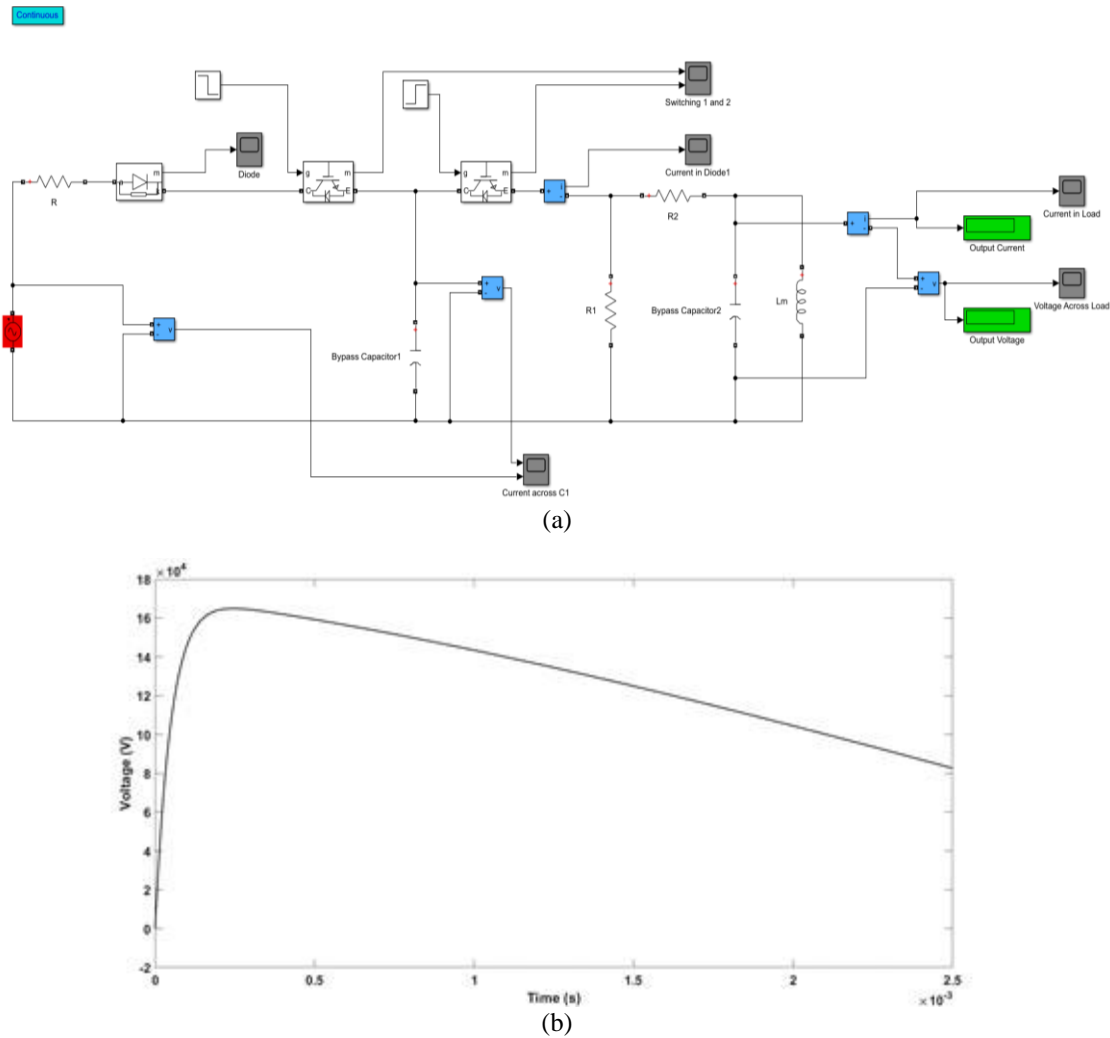


Figure 1. Generating of SSI waveform through impulse generator circuit; (a) generator circuit and (b) 165 kV SSI voltage waveform

Table 1. Impulse generator circuit specification for SSI

Parameters	Units
The leakage inductance, L	0
The primary capacitance, C ₁	10 μF
The wave modulating capacitance, C ₂	1 μF
The modulating inductance, L _m	0.9 H
The current limiting resistor, R	1000 Ω
The wave-tail resistor, R ₁	1155 Ω
The wave-head resistor, R ₂	56 Ω
Amplitude of discharge voltage, U _{c1}	400 V

2.2. The HV winding RLC parameters calculations

The single phase of the winding consists of 96 HV disc windings and 25 LV layered helical windings. The front cross-sectional view of a single-phase winding is illustrated in Figure 2. In addition, the geometrical designations for the HV winding are shown in Table 2.

The RLC elements of the HV disc winding were computed through FEM via quasi-state Ansys Q3D and represented as RLC matrices according to [19]. The R matrix was established as the skin resistance of the winding conductor. The L matrix comprises of self and mutual inductances. The C matrix comprises of turn-to-turn, inter-disc and winding conductor to the ground capacitances. These parameters were computed from the structural specification of the winding using the ANSYS Q3D platform. The capacitances were established through method of moment (MoM) and fast multiple method (FMM) analyses via quasi-electrostatic solver. The AC resistance and inductance were estimated according to MoM via quasi-magnetostatic procedure.

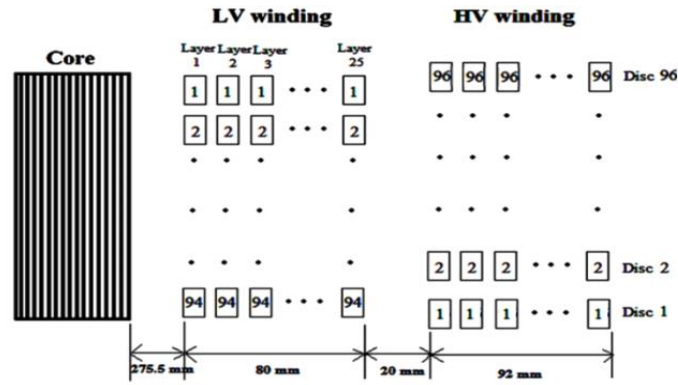


Figure 2. The single-phase disc winding front cross-section view

Table 2. The HV winding geometrical description

Parameters	Values
Number of discs in one phase	96
Number of turns per disc	30
Height of conductor	11.5 mm
Width of the conductor	2.4 mm
The thickness of the insulation (double-sided)	0.5 mm
Distance between each disc	3 mm
Cooling duct between layers 12 and 13	5 mm
Inner radius of the HV winding	374.5 mm
Outer radius of the HV winding	466.5 mm
Total circumference of the HV winding	79.17 mm
Height of HV winding	1437 mm
Insulation between HV-LV windings (9 mm of oil + 1 mm of pressboard)	20 mm

The turn-to-turn and inter-disc capacitances were computed based on MoM and FMM [19]. The turn-to-turn capacitances for every turn has been computed based on [37]. The mutual capacitance, C_m or inter-disc capacitance was calculated based on (1) [38]:

$$C_m = \frac{27.6 \times 1 \times \epsilon_r}{10^{12} \ln\left(\frac{d}{w} + \sqrt{1 - \left(\frac{2w}{d}\right)^2}\right)} F \tag{1}$$

where d is the distance between each disc and w is width of the conductor. ϵ_r is the relative permittivity of the insulation between the turns. The admittance matrix, $[Y] = [G] + j\omega[C]$ which consisted of conductance $[G]$ and capacitance $[C]$ matrices was computed using the quasi-electrostatics solver [39]. The inductance (AC) and resistance (AC) were computed through MoM. The self-inductance, L_{self} was computed using (2):

$$L_{self} = \frac{0.002l \left[\ln\left(\frac{2l}{w+h}\right) + 0.5 + 0.2235\left(\frac{w+h}{l}\right) \right]}{10^6} H \tag{2}$$

where l , h and w are the length, height and width of the winding conductor. The mutual inductance, L_m , exists within two winding conductors whereby one of the conductors is considered as the source that reacts with the neighbouring conductors upon a time-varying magnetic field via quasi magnetostatic interaction [38]. The impedance matrix was presented as $Z = R + j\omega L$. The magnitude of the mutual inductance was computed by (3) based on the coupling factor and conductors length [40]:

$$L_m = \frac{0.002l \left[\ln\left(\frac{2l}{d}\right) - 1 + \left(\frac{d}{l}\right) \right]}{10^6} H \tag{3}$$

where l is the length of conductor and d is the space between the 2 conductors. Because of the skin and proximity effects, the resistance was represented as frequency-dependent and computed using (4) [41]:

$$R = \frac{l}{2\sigma\delta(h+w)} Ohm \tag{4}$$

where l is the length of conductor, σ is the conductors' conductivity and δ represents the conductor skin depth.

The impedance matrices were computed via Ansys Q3D parameter extractor with current as excitation using the quasi-magnetostatics setup. The computed RLC parameters result in 48×48 matrices. The RLC for each of the disc layer was extracted from the matrices as shown in Table 3.

Table 3. RLC parameters of the 8 topmost HV disc winding

Disc	R (mΩ)	L (μH)	C _{ll} (pF)
8	16.4483238	125.90481	8.12728
7	19.5643928	62.032978	8.281119
6	19.6474535	66.438095	8.280154
5	19.6997534	322.64133	8.280349
4	22.3123803	72.702426	8.28092
3	15.4493239	39.693763	8.280631
2	24.4277872	83.315436	8.280979
1	19.6181349	66.35932	8.127188

2.3. The transient resonance due to the SSI

Figure 3 shows the transformer RLC equivalent circuit to compute the transient resonances when subjected to the SSI. The transformer RLC equivalent circuit is presented in Figure 3(a). The schematic diagram of the 96 HV disc winding within the subsystem is shown in Figure 3(b). The analysis was carried out via transient resonance at the time of winding subjected to the switching impulse. The equivalent circuit model validation was performed by a comparison between the calculated and simulated voltage distributions [42].

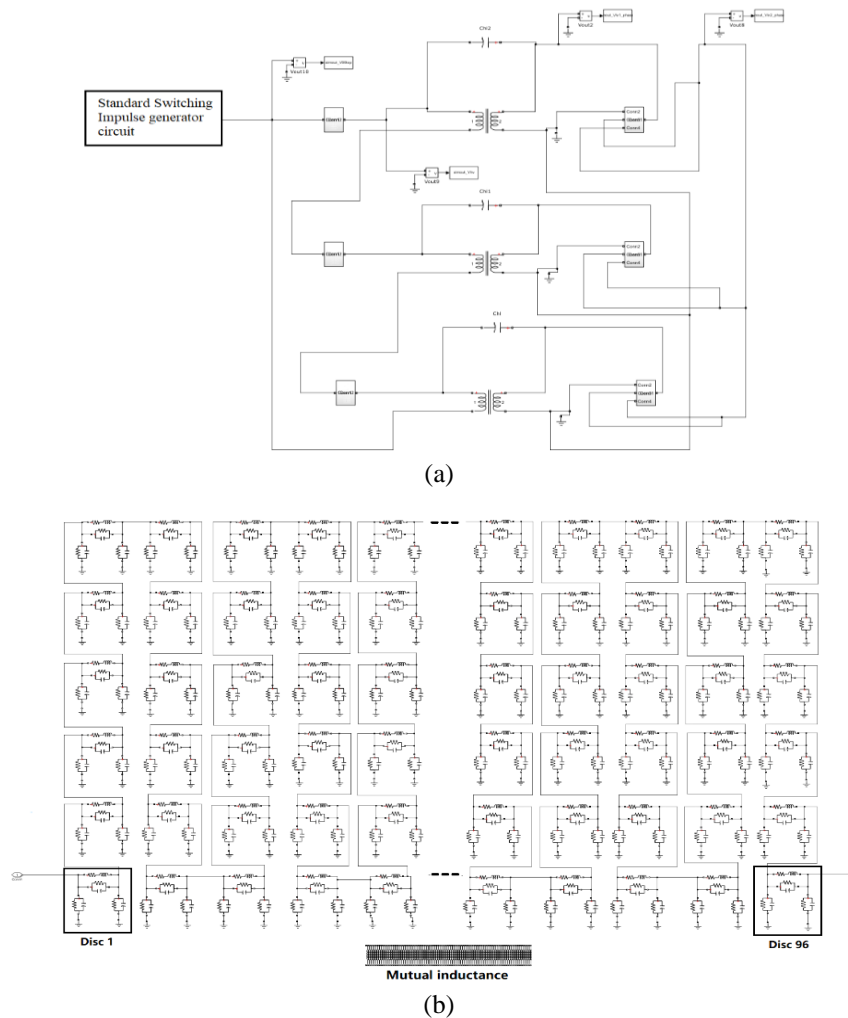


Figure 3. The transformer RLC equivalent circuit to compute transient resonances; (a) transformer RLC equivalent circuit and (b) subsystem of the 96 HV winding

2.4. The axial and radial forces based on analytical method

The analytical method was employed to compute the forces subjected to each of disc layers. The radial F_r and axial F_a directed forces were calculated and estimated according to the winding geometrical design according to (5) and (6) [43].

$$F_r = \frac{2 \times \pi^2 \times (NI)^2 \times D_m \times 10^{-7}}{h} \quad (5)$$

$$F_a = \frac{2 \times \pi^2 \times A \times (NI)^2 \times D_m \times 10^{-7}}{h_{eff}} \quad (6)$$

where h is the length of the winding, h_{eff} is the effective length of the radial flux path, calculated as $0.222 \times h$. D_m is the mean winding diameter, NI is the ampere turn of the winding and A is the winding's total length. The F_r was calculated based on the free distance between two windings as the axial flux density (B_a) between the windings. F_r was assumed to be constant along the length of the windings. It was generated by the integration of the instantaneous ampere-turn (NI) in each of windings as well as the leakage flux derived as (5). The F_a was calculated based on the residual ampere-turns method [44]. It is the relationship between the radial flux density (B_r), the average of ampere-turns at the total length of winding and the effective length of radial flux path (h_{eff}). The magnitudes of axial and radial forces in each disc layer with its leakage fluxes are presented in Table 4.

Table 4. The axial and radial forces in each disc winding

Disc	Voltage dist. (kV)	Fa (mN)	Fr (mN)	Ba (kT)	Br (kT)
8	164.89	88.029	30.858	0.103	1.857
7	164.79	62.157	21.7889	0.087	1.560
6	164.58	61.474	21.549	0.086	1.552
5	164.37	60.990	21.380	0.086	1.546
4	164.15	47.420	16.623	0.076	1.363
3	163.94	38.163	13.378	0.068	1.223
2	163.73	39.358	13.797	0.069	1.242
1	163.52	60.863	21.335	0.086	1.544

2.5. The electromagnetic force analysis based on numerical method

In this case study, only 8 discs were modelled based on an actual geometrical design using Ansys Maxwell to analyse the electromagnetic force experienced by the winding due to switching transient phenomenon. Each of the disc consists of 6 conductors and 5 turns with high-frequency dependent computations. The HV winding geometrical details and RLC elements are shown in Table 2 and Table 3. The properties material of conductor, insulation and boundary were considered as copper, kraft paper and vacuum air. The complete model of the 8 topmost HV disc winding is displayed in Figure 4.

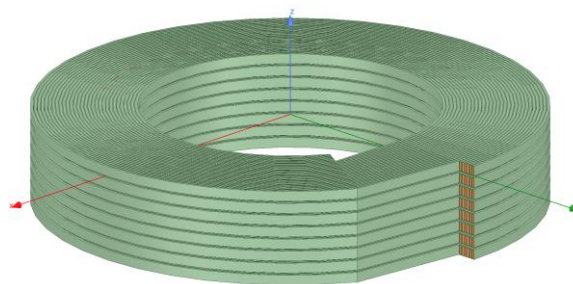


Figure 4. 3D FEM model of 8-disc winding

The electromagnetic solution was carried out in the transient analysis setup. The boundary condition was set as natural and the 165 kV SSI waveform was applied as the excitation on the winding to establish the transient phenomena. The electromagnetic force of the winding was then computed based on the Lorentz force analysis. The meshes were constructed by using adaptive length and skin depth-based refinement techniques to increase the accuracy of forces analysis in the winding. The winding model composes of 926,167 nodes and

369,168 elements. The transient was set from 1 μs to 2500 μs. In the 3D modelling, the calculation of the magnetic plane was defined as (x,y,z) since current was normal to the plane [45]. The component of leakage flux density was expressed as vector potential as in (7) [7],

$$B_x = -\frac{\partial A_\phi}{\partial z}, \quad B_y = 0, \quad B_z = \frac{1}{x} \frac{\partial (xA_\phi)}{\partial x} \tag{7}$$

where B_x, B_y and B_z are directional components of leakage flux density and A_ϕ is the magnetic vector potential. Lorentz force was employed to express the electromagnetic force on the winding as seen in (8) and (9) [6]:

$$F = \int_V J_y \hat{y} \times (B_x \hat{x} + B_z \hat{z}) dv = F_x \hat{x} + F_z \hat{z} \tag{8}$$

$$F_x = B_z \times J_y, \quad F_z = B_x \times J_y \tag{9}$$

where, J_y is the y-directional current density, \hat{x}, \hat{y} and \hat{z} are the unit vectors in the winding plane. The F_x and F_z represent the radial and axial force, respectively.

3. RESULTS AND DISCUSSION

3.1. Transient voltage distribution under SSI

The transient voltage distribution and resonances due to the SSI are shown in Figure 5. V96top is the applied impulse voltage while V96end, V93end, V83end, V73end, V63end and V53end are the voltages at the end of disc layers respectively. The transient resonances at the ends of disc layers indicate slight deviations between 0.41% and 9.04% at the tail time ranging from 350 μs to 2500 μs. The lowest and highest deviations are at V96end and V53end. As the number of disc layers increases, the deviations between V96top and the voltage at the end of disc layers increase, which indicates a decrement in the winding’s stress. The oscillations are influenced by the RLC components in the winding equivalent circuit. The transient voltage distributions along the disc layers initiate resonance oscillations, which causes the stress to build up in the winding.

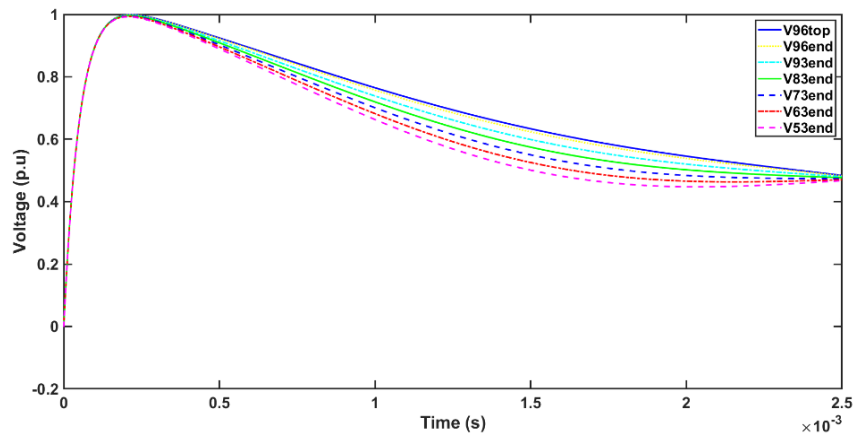


Figure 5. Transient voltage distribution under SSI

3.2. Axial and radial forces based on analytical method

The axial and radial forces computed based on the analytical method via formulated calculations are presented in Figure 6. As seen in Figure 6, the magnitude of the axially directed force on the disc winding is greater than the radially directed force. This is anticipated due to the winding geometrical design. The disc winding structure causes a significant radial leakage flux component to emerge at the ends of the winding, which leads to the increment of the axial force. It is expected that the topmost disc layer, HV disc layer 8 experiences the highest forces and resonances since it is the first layer that is subjected to the SSI. The forces acting on the other disc layers are expected to be uniformly distributed and lower in magnitudes as compared to the topmost disc. However, the forces of disc layers 4, 3, and 2 can decrease due to the RLC parameters in the ampere-turn element of the disc layers.

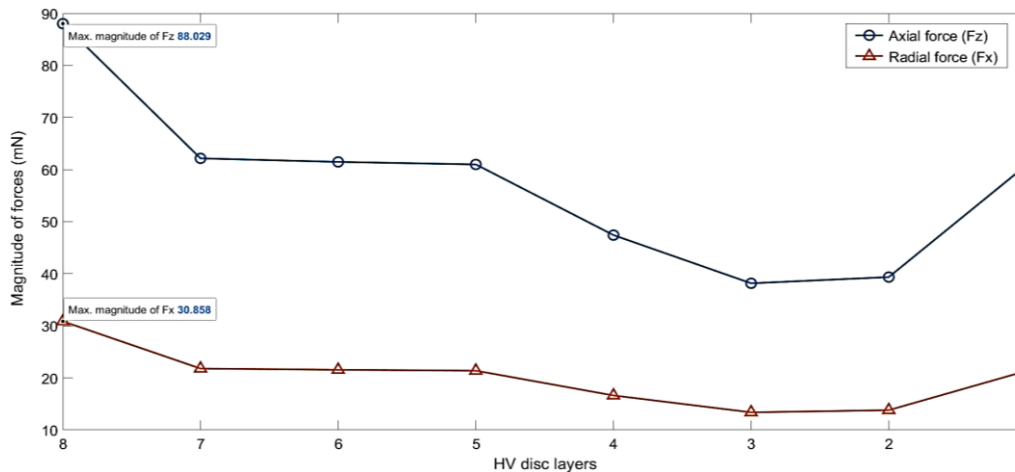


Figure 6. Axial and radial force in disc winding based on calculation

3.3. Electromagnetic forces distribution based on numerical method

The x, y, and z components of the electromagnetic forces based on the numerical method via electric transient analysis in FEM are presented in the time domain as seen in Figure 7. The axial force is seen significantly increases after 1.5 ms. The axial force is in positively directed force towards the HV winding, which represents a tensile force along the disc winding. The peak amplitude of the axially directed force of the HV winding is 35 mN. On the other hand, the radial force gradually increases to a negative amplitude after 1.5 ms. The negatively directed force towards the HV winding indicates that it is an inwardly compressive force. The peak amplitude of the radially directed force on the HV winding is -2.2 mN. The HV disc winding experiences a higher magnitude of axial force as compared to the radial force.

There are differences in the calculated and simulated forces due to the assumptions carried out in the analytical analysis and modelling stage for the numerical analysis. During analytical analysis, the thickness of winding insulation, mutual inductance inter-windings capacitance, spacers between windings, skin and proximity effect are not taken into account while these parameters are considered in the numerical analysis. The consideration of the spacers enhances the relative permittivity and thus increases the inter-disc capacitances for the numerical analysis. Nevertheless, the finding from both methods demonstrates a similar phenomenon which is the HV disc winding experienced higher axially directed force whether in each disc layer or in the overall disc winding when exposed to the SSI.

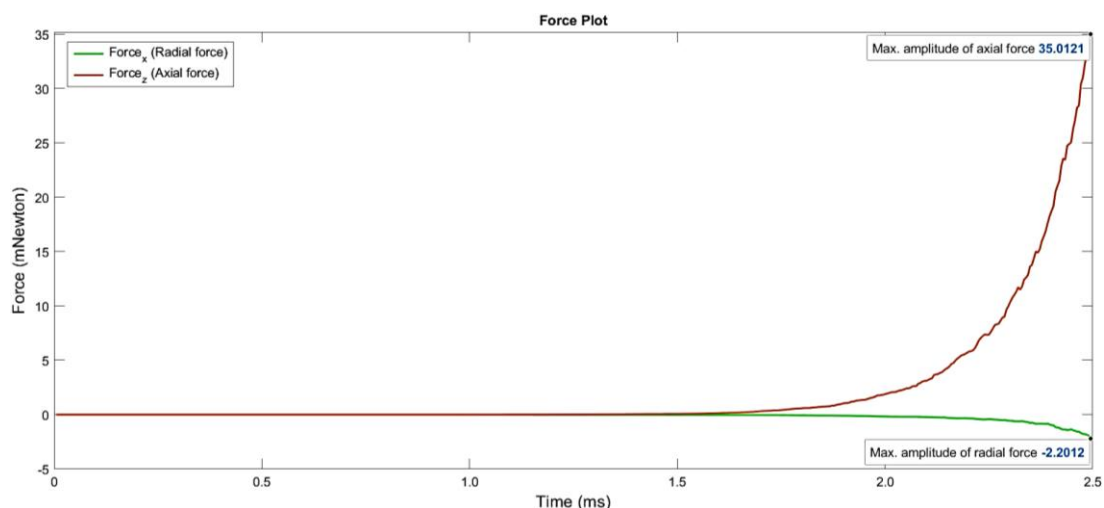


Figure 7. The x (radial) and z (axial) force generated based on FEM

4. CONCLUSION

The study shows that the non-uniform switching impulse voltage distribution results in non-uniform forces distribution along the windings. The axial forces experienced by each disc layer and on the HV disc winding are found to be higher in magnitude as compared to the radial force when subjected to the SSI. The winding electromagnetic force of disc winding is affected by the overall length of the winding as well as the configuration of the winding. This finding would assist the manufacturers on enhancing the radial winding structure during the design stage to minimize the axial force formation on disc-type winding.

ACKNOWLEDGEMENTS

The authors would like to express sincere gratitude to the ALPER UPM for the technical support and the Ministry of Higher Education Malaysia for the funding under the FRGS scheme of FRGS/1/2019/TK07/UPM/02/3 (03-01-19-2071FR).

REFERENCES

- [1] K. C. Agrawal, "Voltage surges—causes, effects and remedies," *Ind. Power Eng. Handb.*, pp. 17-555-17-585, 2001, doi: 10.1016/b978-075067351-8/50095-7.
- [2] B. Li, J. He, Y. Li, and Y. Zheng, "Overvoltage," *Prot. Technol. Ultra-High-Voltage AC Transm. Syst.*, pp. 149–162, Jan. 2020, doi: 10.1016/B978-0-12-816205-7.00009-1.
- [3] C. R. Hall Barbosa, J. Hallstrom, M. T. Silva, L. C. Azevedo, and L. C. Faria, "Estimation of time parameters of tail chopped lightning impulses - Clarification of the standard IEC 60060-1/2010," *CPEM Dig. (Conference Precis. Electromagn. Meas.)* 2014, pp. 778–779, doi: 10.1109/CPEM.2014.6898617.
- [4] M. Arthur *et al.*, "IEEE guide for transformer impulse tests," in *IEEE Standard Association*, no. C57.98-201, New York, 2012, pp. 34–35.
- [5] J. R. Lucas, "High voltage testing," in *High Voltage Engineering*, 2001, pp. 148–165.
- [6] H. M. Ahn, J. Y. Lee, J. K. Kim, Y. H. Oh, S. Y. Jung, and S. C. Hahn, "Finite-element analysis of short-circuit electromagnetic force in power transformer," *IEEE Trans. Ind. Appl.*, vol. 47, no. 3, pp. 1267–1272, 2011, doi: 10.1109/TIA.2011.2126031.
- [7] H. M. Ahn, Y. H. Oh, J. K. Kim, J. S. Song, and S. C. Hahn, "Experimental verification and finite element analysis of short-circuit electromagnetic force for dry-type transformer," *IEEE Trans. Magn.*, vol. 48, no. 2, pp. 819–822, 2012, doi: 10.1109/TMAG.2011.2174212.
- [8] J. C. Das, "Surges transferred through transformers," in *IEEE Conference Record of Annual Pulp and Paper Industry Technical Conference*, 2002, pp. 139–147, doi: 10.1109/papcon.2002.1015142.
- [9] G. B. Kumbhar and S. V. Kulkarni, "Analysis of short-circuit performance of split-winding transformer using coupled field-circuit approach," *IEEE Trans. Power Deliv.*, vol. 22, no. 2, pp. 936–943, 2007, doi: 10.1109/TPWRD.2007.893442.
- [10] J. Lopez-Roldan, M. Popov, L. V. Gool, and J. Declercq, "Analysis, simulation and testing of transformer insulation failures related to switching transient overvoltages," *Present. CIGRE, Paris, Fr.*, vol. 12–116, pp. 1–6, 2002.
- [11] A. Theocharis, M. Popov, R. Seibold, S. Voss, and M. Eiselt, "Analysis of switching effects of vacuum circuit breaker on dry-type foil-winding transformers validated by experiments," *IEEE Trans. Power Deliv.*, vol. 30, no. 1, pp. 351–359, 2015, doi: 10.1109/TPWRD.2014.2327073.
- [12] J. Smajic *et al.*, "Simulation and measurement of lightning-impulse voltage distributions over transformer windings," *IEEE Trans. Magn.*, vol. 50, no. 2, pp. 553–556, 2014, doi: 10.1109/TMAG.2013.2283061.
- [13] T. Zupan, B. Trkulja, R. Obrist, T. Franz, B. Cranganu-Cretu, and J. Smajic, "Transformer windings' RLC Parameters calculation and lightning impulse voltage distribution simulation," *IEEE Trans. Magn.*, vol. 52, no. 3, pp. 2–5, 2016, doi: 10.1109/TMAG.2015.2481004.
- [14] A. Shintemirov, W. H. Tang, and Q. H. Wu, "A hybrid winding model of disc-type power transformers for frequency response analysis," *IEEE Trans. Power Deliv.*, vol. 24, no. 2, pp. 730–739, 2009, doi: 10.1109/TPWRD.2008.2007028.
- [15] G. Liang, H. Sun, X. Zhang, and X. Cui, "Modeling of transformer windings under very fast transient overvoltages," *IEEE Trans. Electromagn. Compat.*, vol. 48, no. 4, pp. 621–627, 2006, doi: 10.1109/TEMC.2006.884537.
- [16] K. Trela and K. M. Gawrylczyk, "Frequency response modeling of power transformer windings considering the attributes of ferromagnetic core," *2018 Int. Interdiscip. PhD Work. IIPhDW 2018*, no. 4, pp. 71–73, 2018, doi: 10.1109/IIPhDW.2018.8388328.
- [17] H. Zhang *et al.*, "Dynamic deformation analysis of power transformer windings in short-circuit fault by FEM," *IEEE Trans. Appl. Supercond.*, vol. 24, no. 3, pp. 5–8, 2014, doi: 10.1109/TASC.2013.2285335.
- [18] K. Dawood, G. Komurgoz, and F. Isik, "Computation of the axial and radial forces in the windings of the power transformer," *Proc. - 2019 4th Int. Conf. Power Electron. their Appl. ICPEA 2019*, no. September, pp. 25–27, 2019, doi: 10.1109/ICPEA1.2019.8911132.
- [19] A. S. Murthy, N. A. Id, and J. Jasni, "Extraction of winding parameters for 33 / 11 kV, 30 MVA transformer based on finite element method for frequency response modelling," *PLoS One*, vol. 8, no. August 27, pp. 1–22, 2020, doi: 10.1371/journal.pone.0236409.
- [20] A. S. Murthy, "Frequency response of transformer winding deformation based on finite element modeling under transient overvoltage impulses," Ph.D dissertation, Dept. Elect. and Elec. Eng., Universiti Putra Malaysia, 2020.
- [21] S. Salon, B. LaMattina, and K. Sivasubramaniam, "Comparison of assumptions in computation of short circuit forces in transformers," *IEEE Trans. Magn.*, vol. 36, no. 5 I, pp. 3521–3523, 2000, doi: 10.1109/20.908881.
- [22] Y. Shibuya and S. Fujita, "High frequency model of transformer winding," *Electr. Eng. Japan*, vol. 146, pp. 8–16, Feb. 2004, doi: 10.1002/eej.10280.
- [23] M. Tahir and S. Tenbohlen, "A comprehensive analysis of windings electrical and mechanical faults using a high-frequency model," *Energies*, vol. 13, no. 1, 2019, doi: 10.3390/en13010105.
- [24] B. Vahidi, N. Ghaffarzadeh, and S. H. Hosseinian, "A wavelet-based method to discriminate internal faults from inrush currents using correlation coefficient," *Int. J. Electr. Power Energy Syst.*, vol. 32, pp. 788–793, doi: 10.1016/j.ijepes.2010.01.015.
- [25] J. Faiz, B. M. Ebrahimi, and T. Noori, "Three- and two-dimensional finite-element computation of inrush current and short-circuit electromagnetic forces on windings of a three-phase core-type power transformer," *IEEE Trans. Magn.*, vol. 44, no. 5, pp. 590–597, 2008, doi: 10.1109/TMAG.2008.917819.

- [26] X. Yan, X. Yu, M. Shen, D. Xie, B. Bai, and Y. Wang, "Calculation of stray losses in power transformer structural parts using finite element method combined with analytical method," *2015 18th Int. Conf. Electr. Mach. Syst. ICEMS 2015*, pp. 320–324, 2016, doi: 10.1109/ICEMS.2015.7385051.
- [27] S. Hasan, S. Taib, S. Hardi, A. Rahim, and A. Shukri, "Core loss characteristics analysis of power transformer under different frequencies excitation," *Proc. 2013 IEEE 7th Int. Power Eng. Optim. Conf. PEOCO 2013*, no. June, pp. 619–623, 2013, doi: 10.1109/PEOCO.2013.6564622.
- [28] A. Bakshi and S. V. Kulkarni, "Analysis of buckling strength of inner windings in transformers under radial short-circuit forces," *IEEE Trans. Power Deliv.*, vol. 29, no. 1, pp. 241–245, 2014, doi: 10.1109/TPWRD.2013.2272102.
- [29] D. Bhalla, R. K. Bansal, and H. O. Gupta, "Analyzing short circuit forces in transformer with single layer helical LV winding using FEM," *2nd Int. Conf. Recent Adv. Eng. Comput. Sci.*, no. 2, pp. 1–6, 2015, doi: 10.1109/RAECS.2015.7453274.
- [30] D. Bhalla, R. K. Bansal, and H. O. Gupta, "Analyzing short circuit forces in transformer for double layer helical LV winding using FEM," *Int. J. Performability Eng.*, vol. 14, no. 3, pp. 425–433, 2018, doi: 10.23940/ijpe.18.03.p3.425433.
- [31] K. Dawood, G. Komurgoz, and F. Isik, "Investigating the effect of axial displacement of transformer winding on the electromagnetic forces," *2020 7th Int. Conf. Electr. Electron. Eng. ICEEE 2020*, 2020, pp. 360–364, doi: 10.1109/ICEEE49618.2020.9102472.
- [32] Vibhuti, G. Walia, and D. Bhalla, "Assessment of the use of FEM for computation of electromagnetic forces, losses and design of transformers," *J. Phys. Conf. Ser.*, vol. 1478, no. 1, 2020, doi: 10.1088/1742-6596/1478/1/012029.
- [33] M. Allahbakhshi, K. Abbaszadeh, and A. Akbari, "Effect of asymmetrical dimensions in short circuit forces of power transformers," *ICEMS 2005 Proc. Eighth Int. Conf. Electr. Mach. Syst.*, vol. 3, no. k 1, pp. 1746–1749, 2005, doi: 10.1109/icems.2005.202858.
- [34] G. B. Kumbhar and S. Mahajan, "The effect of distribution of a primary winding on the short-circuit forces of a current transformer," *Proc. 2017 Int. Conf. Green Energy Appl. ICGEA 2017*, 2017, pp. 153–157, doi: 10.1109/ICGEA.2017.7925474.
- [35] V. Behjat, A. Shams, and V. Tamjidi, "Characterization of power transformer electromagnetic forces affected by winding faults," *J. Oper. Autom. Power Eng.*, vol. 6, no. 1, pp. 40–49, 2018, doi: 10.22098/joape.2018.2436.1210.
- [36] M. Ren, C. Zhang, M. Dong, R. Ye, and R. Albarracín, "A new switching impulse generator based on transformer boosting and insulated gate bipolar transistor trigger control," *Energies*, vol. 9, no. 644, pp. 1–15, 2016, doi: 10.3390/en9080644.
- [37] S. M. A. N. Al-Ameri, M. F. M. Yousof, N. Azis, S. M. Avinash, M. A. Talib, and A. A. Salem, "Modeling frequency response of transformer winding to investigate the influence of RLC," *Indonesian Journal of Electrical Engineering and Computer Science*, vol. 14, no. 1, pp. 219–229, 2019, doi: 10.11591/ijeecs.v14.i1.pp219-229.
- [38] X. Liu, Y. Wang, J. Zhu, Y. Guo, G. Lei, and C. Liu, "Calculation of capacitance in high-frequency transformer windings," *IEEE Trans. Magn.*, vol. 52, no. 7, pp. 14–17, 2016, doi: 10.1109/TMAG.2016.2522976.
- [39] S. M. H. Hosseini, M. Vakilian, and G. B. Gharehpetian, "Comparison of transformer detailed models for fast and very fast transient studies," *IEEE Trans. Power Deliv.*, vol. 23, no. 2, pp. 733–741, 2008, doi: 10.1109/TPWRD.2008.915795.
- [40] M. Popov, L. V. D. Sluis, G. C. Paap, and H. D. Herdt, "Computation of very fast transient overvoltages in transformer windings," *IEEE Trans. Power Deliv.*, vol. 18, no. 4, pp. 1268–1274, 2003, doi: 10.1109/ICEMS12746.2007.4412335.
- [41] X.-C. Wei, *Modeling and design of electromagnetic compability for high-speed printed circuit boards and packaging*, CRC Press. Rosewood Drive, Danvers: Boca Raton, 2017.
- [42] A. S. Murthy *et al.*, "Investigation on the resonant oscillations in an 11 kV distribution transformer under standard and chopped lightning impulse overvoltages with different shield placement configurations," *Energies*, vol. 12, no. 8, 2019, doi: 10.3390/en12081466.
- [43] N. F. M. Yasid, N. Azis, M. F. M. Yousof, M. A. Talib, and A. S. Murthy, "Axial and radial force distributions computation in disc-type winding under switching surge," in *2022 IEEE International Conference in Power Engineering Application (ICPEA)*, no. March, 2022, pp. 1–4, doi: 10.1109/ICPEA53519.2022.9744688.
- [44] A. C. De Azevedo, I. Rezende, A. C. Delaiba, J. C. De Oliveira, B. C. Carvalho, and S. B. De Herivelto, "Investigation of transformer electromagnetic forces caused by external faults using FEM," *2006 IEEE PES Transmission and Distribution Conference and Exposition: Latin America, TDC'06*. 2006, doi: 10.1109/TDCLA.2006.311522.
- [45] M. R. Feyzi and M. Sabahi, "Finite element analyses of short circuit forces in power transformers with asymmetric conditions," *IEEE Int. Symp. Ind. Electron.*, no. 1, pp. 576–581, 2008, doi: 10.1109/ISIE.2008.4677272.

BIOGRAPHIES OF AUTHORS



Nurul Farahwahida Md Yasid     obtained her B.Eng. and M.Eng. Degrees in Electrical Engineering from Universiti Tun Hussein Onn Malaysia (UTHM) in 2017 and 2019, respectively. She is currently pursuing Ph.D degree in Electrical Power Engineering at Universiti Putra Malaysia. Her research interest includes the high voltage equipment and condition monitoring of transformers using the frequency response analysis (FRA), finite element method (FEM) and more. She can be contacted at email: gs60248@student.upm.edu.my or farahwahida.yasid@gmail.com.



Assoc. Prof. Ir. Dr. Norhafiz Azis     received the B.Eng. degree in electrical and electronic engineering from Universiti Putra Malaysia, Serdang, Malaysia, in 2007, and the Ph.D. degree in electrical power engineering from The University of Manchester, Manchester, U.K. He is currently an Associate Professor with the Department of Electrical and Electronic Engineering, Universiti Putra Malaysia. His research interests are in-service aging of transformer insulation, condition monitoring, asset management, and alternative insulation materials for transformers. He can be contacted at email: norhafiz@upm.edu.my.



Assoc. Prof. Ir. Dr. Mohd Fairouz Mohd Yusof    obtained B. Eng and M. Eng from Universiti Teknologi Malaysia. He completed his Ph.D. study from The University of Queensland, Australia and currently is an Associate Professor under the Department of Electrical Power Engineering, Universiti Tun Hussein Onn Malaysia (UTHM). His main research is condition-based monitoring and assessment of power transformers and rotating machines. He can be contacted at email: fairouz@uthm.edu.my.



Assoc. Prof. Dr. Jasronita Jasni    received the B.Eng. degree in electrical engineering and the M.Eng. degree in electrical engineering from Universiti Teknologi Malaysia, Johor Bahru, Malaysia, in 1998 and 2001, respectively, and the Ph.D. degree in electrical power engineering from Universiti Putra Malaysia, Serdang, Malaysia, in 2010. She is currently an Associate Professor with the Department of Electrical and Electronic Engineering, Universiti Putra Malaysia. Her research interests include power system analysis for static and dynamics, load flow analysis, embedded generation, and renewable energy. She can be contacted at email: jas@upm.edu.my.



Ir. Dr. Mohd Aizam Talib    received his B.Eng in Electrical Engineering from the University of Portsmouth, UK in 1997, M.Eng in Electrical Engineering from Universiti Tenaga Nasional (UNITEN), Malaysia in 2001 and Ph.D degree at Universiti Teknologi Malaysia in 2016. He has over 24 years of experience in dealing with transformer research, testing, diagnostic and life assessment of in-service power transformers. He has held several positions previously with TNB Research Sdn Bhd as Senior Research Engineer, Manager for High Voltage Testing Laboratory and Senior Technical Expert (Transformer). Presently, he is Head of Advanced Diagnostic Services at TNB Labs Sdn Bhd. His research interests are in transformer condition monitoring, insulation diagnostic and dielectric measurements. He can be contacted at email: aizam.talib@tnb.com.my.



Dr. Avinash Srikanta Murthy    received B.Eng. in Electrical and Electronics Engineering from Malnad College of Engineering in 2011. He received M.Tech. in Power and Energy Systems from National Institute of Technology Karnataka, Surathkal in 2013. He then received his Ph.D degree in Electrical Power Engineering from Universiti Putra Malaysia (UPM) in 2020. He is working as an R&D Engineer at Transformer Technology Centre, Hitachi Energy, India. His research is on high voltage testing, transformer deformation analysis using frequency response analysis and simulation using computational electromagnetics, ansys electromagnetics and workbench, MATLAB, COMSOL multiphysics and C. He can be contacted at email: avinash.murthy@hitachienergy.com.